AD-A150 922 ANALYTICAL STUDIES AND EXPERIMENTAL MEASUREMENTS OF AMPLITUDE AND PHASE O.. (U) KANSAS UNIV/CENTER FOR RESEARCH INC LAWRENCE REMOTE SENSING L.. A W BIGGS 1/1

UNCLASSIFIED MAY 84 CRINC/RSL-TR-6190-F AFOSR-TR-85-0119 F/G 20/14 NL

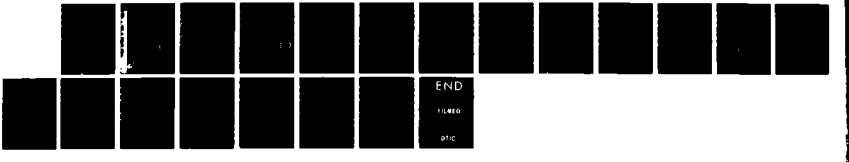

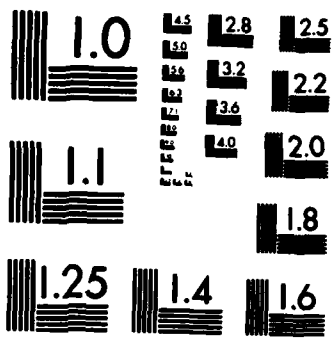

MICROCOPY RESOLUTION TEST CHART
NATIONAL BUREAU OF STANDARDS-1963-A

(2)

CRINC

REMOTE SENSING LABORATORY

ANALYTICAL STUDIES AND EXPERIMENTAL MEASUREMENTS OF AMPLITUDE AND PHASE OF NEAR-FIELD RANGE ANTENNA PROBES

Final Report

THE UNIVERSITY OF KANSAS CENTER FOR RESEARCH, INC.
2291 Irving Hill Drive—Campus West
Lawrence, Kansas 66045

Unclassified
SECURITY CLASSIFICATION OF THIS PAGE

REPORT DOCUMENTATION PAGE

1a. REPORT SECURITY CLASSIFICATION: Unclassified	1b. RESTRICTIVE MARKINGS: None
2a. SECURITY CLASSIFICATION AUTHORITY	3. DISTRIBUTION/AVAILABILITY OF REPORT: Approved for public release; distribution unlimited.
2b. DECLASSIFICATION/DOWNGRADING SCHEDULE	
4. PERFORMING ORGANIZATION REPORT NUMBER(S): RSL TR 6190-Final	5. MONITORING ORGANIZATION REPORT NUMBER(S): AFOSR-TR- 85-0119
6a. NAME OF PERFORMING ORGANIZATION: University of Kansas Center for Research, Inc. / 6b. OFFICE SYMBOL (If applicable)	7a. NAME OF MONITORING ORGANIZATION: AFOSR/NE
6c. ADDRESS (City, State and ZIP Code): 2291 Irving Hill Drive Lawrence, Kansas 66045	7b. ADDRESS (City, State and ZIP Code): Bldg 410 Bolling AFB DC 20332-6448
8a. NAME OF FUNDING/SPONSORING ORGANIZATION: AFOSR / 8b. OFFICE SYMBOL (If applicable): NE	9. PROCUREMENT INSTRUMENT IDENTIFICATION NUMBER: AFOSR-83-0190
8c. ADDRESS (City, State and ZIP Code): Bolling AFB, D.C. 20332	10. SOURCE OF FUNDING NOS.

PROGRAM ELEMENT NO.	PROJECT NO.	TASK NO.	WORK NO
61102F	2305	D9	

11. TITLE (Include Security Classification): Analytical Studies & Experimental Measurements

12. PERSONAL AUTHOR(S): Biggs, Albert W.

13a. TYPE OF REPORT	13b. TIME COVERED	14. DATE OF REPORT (Yr., Mo., Day)	15. PAGE COUNT
FINAL	FROM 83/05/01 TO 84/06/30	84/05	16

16. SUPPLEMENTARY NOTATION

17. COSATI CODES			18. SUBJECT TERMS (Continue on reverse if necessary and identify by block number)
FIELD	GROUP	SUB. GR.	Probe antennas, directional effects, computed patterns, amplitude and phase, near-field range, Lorentz reciptocity

19. ABSTRACT (Continue on reverse if necessary and identify by block number)

The effects of probe antenna errors in the basic theory of probe compensated near-field measurements for arbitrary antenna are presented. The study encompassed: (1) measurements made in the near-field of the arbitrary test antenna; (2) directional effects of probe antennas on reception by test antennas; and (3) computed patterns of test antennas that span a solid angle instead of one or two principal plane cuts. Results of experimental measurements conducted are reported with both advantages and disadvantages discussed. Fields from the test and probe antennas are expressed in elementary plane wave expansions and the Lorentz reciptrocity theorem is used to calculate the output.

20. DISTRIBUTION/AVAILABILITY OF ABSTRACT	21. ABSTRACT SECURITY CLASSIFICATION
UNCLASSIFIED/UNLIMITED ☐ SAME AS RPT. ☒ DTIC USERS ☐	Unclassified

22a. NAME OF RESPONSIBLE INDIVIDUAL	22b. TELEPHONE NUMBER (Include Area Code)	22c. OFFICE SYMBOL
ROBERT W CARTER, Lt Col, USAF	(202) 767-4931	NE

DD FORM 1473, 83 APR

Unclassified

ANALYTICAL STUDIES AND EXPERIMENTAL MEASUREMENTS OF AMPLITUDE AND PHASE OF NEAR-FIELD RANGE ANTENNA PROBES

Final Report

Prepared by
Albert W. Biggs
Principal Investigator

Remote Sensing Laboratory
University of Kansas Center for Research, Inc.
Lawrence, Kansas 66045-2969

RSL-TR 6190-F~~inal~~

May 1984

Supported by

Air Force Office of Scientific Research
Bolling Air Force Base
Washington, D.C. 20332

Contract No. AFOSR-83-0190

INTRODUCTION

The purpose of this study is to present the effect of probe antenna errors in the basic theory of probe compensated near-field measurements for arbitrary antennas. Major features of this basic theory include the following.

(1) Measurements are made in the near-field of the arbitrary test antenna.

(2) Directional effects of probe antennas on reception by test antennas are included.

(3) Computed patterns of test antennas span a solid angle instead of one or two principal plane cuts.

Experimental measurements include three parts.

(1) The probe antenna is described by the amplitude and phase of its antenna pattern. This is equivalent to a "transfer function" from a systems theory approach. The antenna pattern of the probe antenna is calculated from a theoretical model, or measured in a suitable far-field antenna range. Errors in amplitude and phase of the calculated or measured antenna pattern were not significant with conventional test antennas. They become significant with adaptive and low sidelobe antenna arrays, where sidelobe levels are 30-50 dB below mainlobe maxima.

(2) The tangential fields are measured at preselected intervals on a prescribed planar surface in the near-field of the test antenna. These measurements are made with two orthogonal orientations of the probe antenna.

(3) The far-fields of the test antenna with the Fast Fourier Transform (FFT) or a similar algorithm. If pattern details over a

predetermined solid angle are desired, filtering can achieve better resolution.

Advantages of probe-compensated near-field measurements are described below.

(1) They are time and cost effective. Accuracies of calculated patterns are equal to or better than those for far-field antenna ranges.

(2) Near-field antenna ranges are all-weather facilities. Far-field antenna ranges have environments changing from dry snow over frozen soil in winter to soggy or wet soil in summer. Many roof-top far-field antenna ranges sometimes have transient pools of water or ice. They also may have man-made obstacles in the form of antenna cables, power lines, and adjacent buildings.

(3) When large antenna arrays are tested, far-field range size limitations, transportation, mounting problems, and requirements for large-scale positioners are not present.

There are also disadvantages to be included in a decision to develop a near-field antenna range.

(1) More complex and expensive measurement facilities are required.

(2) More careful and precise methods are required to calibrate the near-field probe antennas in comparison with far-field probe antennas.

(3) Since test antenna patterns are not obtained in real time, a suitable algorithm is required to transform the measurements into a usable form.

(4) Computer software is very important for the above transforms.

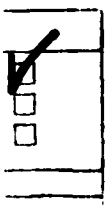

Near-field measurements on planar surfaces, in front of the test antenna, are more prevalent [1-4] because of their mathematical and computational features. Their disadvantage is a limitation of the pattern calculation in a cone with an apex angle less than 180° without a repetition of measurements. This limitation is partially avoided with cylindrical measurement surfaces [5,6]. The complete 180° azimuth pattern for all elevation angles (but not including spherical polar angles) can be obtained with one measurement [7] with spherical measurement surfaces. This is most attractive because a complete 4π steradian pattern is computed from a single measurement, but computations are extremely difficult except for test antennas with broad-beam patterns. The planar and cylindrical surfaces have computational advantages because of the FFT algorithm. Spherical surfaces cannot utilize this algorithm.

In the third section, fields from the test and probe antennas are expressed in elementary plane wave expansions. The Lorentz reciprocity theorem, with the test antenna as the reciever and the probe antenna as the source, is then introduced [5] to calculate the test antenna output as a function of the expanded fields. The result is an algebraic equation which relates the known field of the probe antenna to the unknown field received by the test antenna.

NEAR-FIELD ANTENNA RANGES

Most of the experimental measurements made on antenna arrays relate to the fundamental characteristics of these arrays which determine their immediate application. Some of these characteristics are input impedances, far-field antenna array patterns, far-field antenna element patterns, mutual

coupling between elements, influence of frequency variations on the preceding characteristics and efficiencies or gains. However, there are occasions when it is necessary to have information about current and charge distributions on the antenna array elements, and the distributions of near-fields in the immediate vicinity of the array.

Antenna array near-fields are divided into the "reactive near-field" and the "radiating near field" [8]. The reactive near-field surrounds the immediate region of the antenna, and must satisfy the inequality [9]

$$.62\sqrt{D^3/\lambda} > z_0 > 0 \tag{1}$$

where D is the largest dimension of the test antenna array (also referred to as simple "test antenna"), λ is the wavelength of the signal transmitted from the test antenna, and $z = z_0$ is the planar surface on which the probe antenna moves. The planar surface at z_0 indicates the coordinate system in this study. It was chosen so that the plane or aperture coincides with the x-y plane at $z = 0$. The distance z_0 must also satisfy the inequality

$$z_0 > \frac{2d^2}{\lambda} \tag{2}$$

where d is the largest dimension of the probe antenna. This inequality places the test antenna in the far-field of the probe antenna. Inequalities in Equations (1) and (2) may be combined in the form

$$0.62\sqrt{D^3/\lambda} > z_0 > \frac{2d^2}{\lambda} \tag{3}$$

so that the probe antenna is always in the reactive near-field of the test antenna, while the test antenna is always in the far-field of the probe antenna.

NEAR-FIELD PROBE ANTENNA COMPENSATION

The theory of probe compensated measurements on planar surfaces is based on expansion of the test and probe antenna fields into elementary plane waves or modes [10]. The modes are an angular spectrum of plane waves [11]. The Lorentz reciprocity theorem is then applied [5] to obtain probe output which relates the known probe field to the unknown radiated test antenna fields. The unknown modal amplitudes are then found with this equation. The far-field antenna pattern is finally calculated from the modal amplitudes.

Any arbitrary monochromatic wave may be seen as a superposition of plane waves. They have the same frequency, but travel in different directions with different amplitudes. Plane wave expansions are made to find the unknown amplitudes and directions of the plane waves. The resulting summation of these waves is a modal expansion of the original arbitrary wave.

In a linear, homogeneous, isotropic, and charge free region, and with a harmonic time dependence exp ($j\omega t$), Maxwell's equations yield the vector Helmholtz equation for the electric field $\vec{E}$. In free space, the electric field has the form,

$$\vec{E} = \vec{A}\,(\vec{k})\; e^{-j\,\vec{k}\,\cdot\,\vec{r}} \qquad (4)$$

where $\vec{A}\,(\vec{k})$ is the plane wave spectrum with the propagation constant k,

$$\vec{k} \cdot \vec{k} = k^2 = k_x^2 + k_y^2 + k_z^2 \tag{5}$$

so that the component k_z is

$$k_z = \sqrt{k^2 - k_x^2 - k_y^2}\,, \; k^2 > k_x^2 + k_y^2, \; = -j\sqrt{k_x^2 + k_y^2 - k^2}, \; k^2 < k_x^2 + k_y^2 \tag{6}$$

General solutions for $\vec{E}\,(\vec{r})$ are formed by summing over all k_x and k_y,

$$\vec{E}\,(\vec{r}) = \int \int_{-\infty}^{\infty} \vec{A}\,(\vec{k})\, e^{-j\,\vec{k} \cdot \vec{r}}\, dk_x dk_y. \tag{7}$$

Since Eq. (7) is the inverse Fourier transform of components A_x and A_y, then

$$\vec{A}\,(\vec{k}) = \frac{e^{jk_z z_o}}{4\pi^2} \int \int_{-\infty}^{\infty} \vec{E}\,(x,y,z_o) e^{j(k_x x + k_y y)}\, d\,x\, dy, \tag{8}$$

on the plane $z = z_o$. The vector expression in Eq. (8) includes A_x and A_y components for E_x and E_y, respectively. The saddle point method yields [12]

$$\vec{E}\,(\vec{r}) = j\,\frac{2\pi}{r}\,k_z\,\vec{A}\,(\vec{k})\, e^{-jkr} \tag{9}$$

where, in rectangular coordinates,

$$\vec{k} = \hat{k}r = k \sin\theta \cos\phi\, \hat{x} + k \sin\theta \sin\phi\, \hat{y} + k \cos\theta\, \hat{z} \tag{10}$$

and where $\hat{k}$, $\hat{x}$, $\hat{y}$, and $\hat{z}$ are unit vectors.

If the tangential fields on a planar surface are known, the plane wave spectrum can be calculated. The plane wave spectrum provides the spatial

field distribution. This result is achieved because far-field antenna patterns and their near-field aperture distributions are Fourier transforms of each other [3]. When a probe antenna is a source of tangential fields from the planar surface, the fields are perturbed by the probe and test antenna interactions so that the actual planar distribution is never seen. If negligible interaction between probe and test antennas is assumed, probe perturbations can be compensated with application of the Lorentz reciprocity theorem.

Figure 1 is the coordinate system for the test and probe antennas. Fields radiated by the probe antenna are measured by the test antenna at predetermined increments while the probe antenna moves across the $z = z_0$ plane. The receiving pattern of the test antenna is [13]

$$\vec{R}\ (\theta,\phi) = R_\theta\ (\theta,\phi)\ \hat{\theta} + R_\phi\ (\theta,\phi)\ \hat{\phi}, \tag{11}$$

where coordinates (θ,ϕ) at the center of the test antenna define directions from which uniform waves are incident on the antenna, and where $\hat{\theta}$ and $\hat{\phi}$ are unit vectors. If the vector amplitude of the plane wave spectrum from the probe antenna is $\vec{E}$, the received voltage $v(\theta,\phi)$ at the test antenna terminals is

$$v(\theta,\phi) = \vec{R} \cdot \vec{E} = R_\theta E_\theta + R_\phi E_\phi, \tag{12}$$

indicating dependence of the received signal on polarization and direction of the incident waves.

Since the test antenna is radiated by the probe antenna in the test antenna near-field, the received signal does not have the form of Eq. (12),

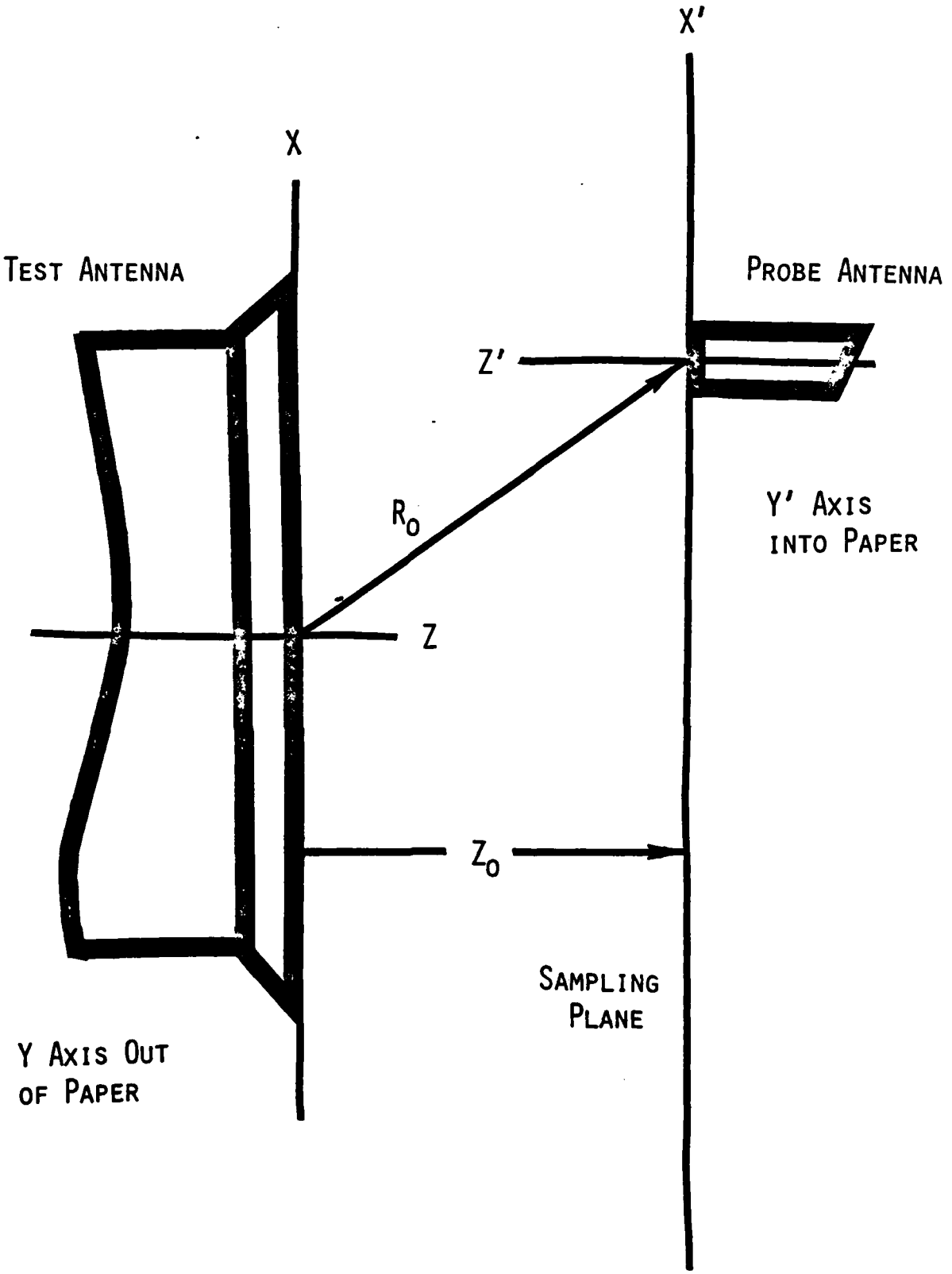

FIGURE 1. NEAR-FIELD ANTENNA RANGE COORDINATE SYSTEM.

The probe antenna radiates a spherical wave, or a spectrum of plane waves, so that the received voltage is a superposition of voltages from each component in the plane wave spectrum of the probe antenna. The integrated sum of the received voltage $v(\vec{r}_o)$ is

$$v(\vec{r}_o) = \int_{-\infty}^{\infty} \vec{R}(\theta,\phi) \cdot \vec{A}(\vec{k})\, e^{-j\vec{k} \cdot \vec{r}_o}\, dk_x dk_y, \tag{13}$$

similar to Eq. (7) with $\vec{r}_o$ equal to

$$\vec{r}_o = x\hat{x} + y\hat{y} + z_o\hat{z}. \tag{14}$$

Primes (') will indicate the probe antenna coordinate system (they were omitted for purposes of clarity) in subsequent equations, while unprimed coordinates relate to the test antenna coordinate system. The spectrum $\vec{A}(\vec{k}')$ is the spectrum from the probe antenna, so that with Eq. (9),

$$\vec{E}(\vec{r}') = j\frac{2\pi}{r'} k_z' \vec{A}(\vec{k}')\, e^{-jkr'}, \tag{15}$$

represents the electric field in the far-field of the probe antenna. Since, from Eq. (10), k_z' is $k'\cos\theta'$, Eq. (12) becomes

$$\vec{E}(\vec{r}') = C \cos\theta' \vec{A}(\vec{k}'), \tag{16}$$

where $j2\pi k' \exp(-jk'r')/r'$ equals the constant C because it is assumed that the far-field probe antenna pattern is specified on a sphere of constant radius.

Equation (13) is a two-dimensional Fourier transform in transform space. Its inverse transform in physical space is

$$\vec{R}\,(\theta,\phi) \cdot \vec{A}\,(\vec{k}') = \int_{-\infty}^{\infty}\int v\,(\vec{r}_o)\, e^{j\vec{k}\cdot\vec{r}_o}\, dxdy, \qquad (17)$$

similar to Eq. (8). With Eq. (16), but in test antenna coordinates [10],

$$\begin{aligned}\vec{R}\,(\theta,\phi) \cdot \vec{E}\,(\vec{r}') &= [R_\theta(\theta,\phi)\hat{\theta} + R_\phi(\theta,\phi)\hat{\phi}] \cdot \\ &\quad [E_{\theta'}(\theta',\phi')\hat{\theta} + E_{\phi'}(\theta',\phi')\hat{\phi}'] \\ &= [R_\theta(\theta,\phi)\hat{\theta} + R_\phi(\theta,\phi)\hat{\phi}] \cdot \\ &\quad [-E_\theta(\theta,\pi-\phi)\hat{\theta} - E_\phi(\theta,\pi-\phi)\hat{\phi}] \\ &= -R_\theta(\theta,\phi)E_\theta(\theta,\pi-\phi) - R_\phi(\theta,\phi)E_\phi(\theta,\pi-\phi) \\ &= -I(\theta,\phi)\cos\theta, \qquad (17)\end{aligned}$$

where the integral $I(\theta,\phi)$ is

$$I(\theta,\phi) = -Ce^{jk_z z_o} \int_{-\infty}^{\infty}\int v\,(x,y,z_o)\, e^{j(k_x x + k_y y)}\, dxdy. \qquad (18)$$

The probe coordinates are changed to test antenna coordinates with

$$\hat{\theta}' = -\hat{\theta},\ \hat{\phi}' = -\hat{\phi},\ \theta' = \theta,\ \phi' = \pi - \phi. \qquad (19)$$

An alternative form for Eq. (18), in terms of detected probe output $P(x,y,z_o)$ is

$$I(\theta,\phi) = e^{jk_z z_o} \int_{-\infty}^{\infty}\int P(x,y,z_o)\, e^{j(k_x x + k_y y)}\, dxdy, \qquad (20)$$

where $P(x,y,z_o) = -C\, v(x,y,z_o)$.

In a near-field aperture measurement, both horizontally and vertically polarized fields are radiated by the probe so that two expressions are obtained for the desired far-field functions of the test antenna. The detected probe outputs are then given by $P_V(x,y,z_o)$ and $P_H(x,y,z_o)$, where subscripts V and H are vertical and horizontal polarizations, respectively. The expressions for both polarizations in Eq. (17) are

$$R_\theta(\theta,\phi)\, E_\theta^V(\theta,\phi) + R_\phi(\theta,\phi)\, E_\phi^V(\theta,\phi) = I_V \cos\theta,$$

$$R_\theta(\theta,\phi)\, E_\theta^H(\theta,\phi) + R_\phi(\theta,\phi)\, E_\phi^H(\theta,\phi) = I_H \cos\theta, \qquad (21)$$

and when combined to obtain the far-field components of the test antenna,

$$R_\theta = \cos\theta\, \frac{I_V E_\phi^H - I_H E_\phi^V}{\Delta(\theta,\phi)} \qquad (22)$$

$$R_\phi = \cos\theta\, \frac{I_H E_\theta^V - I_V E_\theta^H}{\Delta(\theta,\phi)} \qquad (23)$$

where the determinant $\Delta(\theta,\phi)$ is

$$\begin{vmatrix} E_\theta^V & E_\phi^V \\ E_\theta^H & E_\phi^H \end{vmatrix} = E_\theta^V E_\phi^H - E_\phi^V E_\theta^H, \qquad (24)$$

with (θ,ϕ) and $(\theta,\pi-\phi)$ omitted for clarity.

The functions $I_V(\theta,\phi)$ and $I_H(\theta,\phi)$ are expressed as

$$I_V(\theta,\phi) = e^{jkz_o\cos\theta} \int_{-\infty}^{\infty}\int P_V(x,y,z_o) \cdot e^{jk(x\sin\theta\cos\phi + y\sin\theta\sin\phi)}dxdy, \quad (25)$$

$$I_H(\theta,\phi) = e^{jkz_o\cos\theta} \int_{-\infty}^{\infty}\int P_H(x,y,z_o) \cdot e^{jk(x\sin\theta\cos\phi + y\sin\theta\sin\phi)}dxdy. \quad (26)$$

SPATIAL SAMPLING IN NEAR-FIELD RANGES

Planar arrays are usually located with their back side parallel to an interior wall, or parallel to an interior floor, with the array axis parallel to the floor. A typical envelope of a test antenna is a planar array with dimensions of 1 meter by 7 meters. The planar measurement surface is arbitrarily chosen to be 5 - 10 wavelengths from the array surface. With a frequency range 3 - 4 GHz, the wavelength is thus 7.5 - 10 cm, so the distance z_o becomes 0.75 - 1.00 meter.

The planar measurement surface has a coordinate system where the vertical (up) direction is the positive y-axis, the positive z-axis is normal from the planar surface (toward the probe antenna), and the positive z-axis moves to the right in front of the planar surface in a horizontal direction. The width and height of the sampling surface are X and Y, respectively. The planar surface is also called the sampling surface because the probe antenna moves horizontally across the surface in sequential vertical increments.

Two sets of measurements are made at a finite number of equally spaced intervals along the x- and y-axes so that Eqs. (25) and (26) can be

numerically evaluated with the FFT algorithm. The sampling plane is divided into a grid of points with coordinates

$$(m\Delta x,\ n\Delta y,\ z_0), \tag{27}$$

at wave numbers defined by discrete Fourier transform theory,

$$\begin{aligned} k_x &= \frac{2m\pi}{M\Delta x},\ -\frac{M}{2} < m < \frac{M}{2} - 1, \\ k_y &= \frac{2n\pi}{N\Delta y},\ -\frac{N}{2} < n < \frac{N}{2} - 1. \end{aligned} \tag{28}$$

The rectangular grid has M ordinates in the x-direction, with a width $(M-1)\Delta x$, and N abscissas in the y-direction for a height or length $(N-1)\Delta y$. The total number of grid intersections is MN. At each point, the spherical coordinates θ, ϕ are found with

$$\begin{aligned} \cos\phi &= \frac{mN\lambda\Delta y}{\sqrt{(mN\Delta y)^2 + (nM\Delta x)^2}}, \\ \sin\theta &= \lambda\sqrt{\left(\frac{m}{M\Delta x}\right)^2 + \left(\frac{n}{N\Delta y}\right)^2}\ . \end{aligned} \tag{29}$$

The spacings Δx and Δy are selected by the attenuation desired for evanescent waves [3],

$$\alpha = 54.6\ L\ \left[\left(\frac{\lambda}{\Delta s}\right)^2 - 1\right]^{1/2}\ \text{dB}, \tag{30}$$

where $\Delta s = \Delta x = \Delta y$, and L is the number of wavelengths between the planar and array surfaces, $z_0 = L\lambda$.

ERRORS IN FAR-FIELD PATTERN CALCULATIONS

At microwave frequencies, the conventional antenna probe is usually an open-end rectangular waveguide [14]. The antenna probe usually transmits in its lowest mode, TE_{10}, where

$$E_\theta = -\frac{n(\pi ab)^2 \sin\theta}{2\lambda^3 r\,(\frac{\pi}{a})^2}\left[1 + \frac{\beta_{10}}{k}\cos\theta + \rho(1 - \frac{\beta_{10}}{k}\cos\theta)\right]\left[(\frac{\pi}{a})^2 \sin^2\phi\right] \Psi_{10}(\theta,\phi), \tag{31}$$

$$E_\phi = \frac{n(\pi ab)^2 \sin\theta\sin\phi\cos\phi}{2\lambda^3 r}\cdot \left[\cos\theta + \frac{\beta_{10}}{k} + p(\cos\theta - \frac{\beta_{10}}{k})\right] \Psi_{10}(\theta,\phi), \tag{32}$$

where

$$\Psi_{10}(\theta,\phi) = \frac{\sin(\frac{1}{2}ka\,\sin\theta\cos\phi + \frac{\pi}{2})}{(\frac{1}{2}ka\,\sin\theta\cos\phi)^2 + (\frac{\pi}{2})^2}\cdot \frac{\sin(\frac{1}{2}kb\,\sin\theta\,\sin\phi)}{(\frac{1}{2}kb\,\sin\theta\,\sin\phi)^2}, \tag{33}$$

where a and b are the waveguide internal dimensions, with $a > b$. Errors in the far-field antenna pattern occur when incorrect values of a and b are introduced into Eqs. (31) - (33). These are measurement errors. Polarization errors create far-field pattern errors if there are deviations from correct alignment of the probe for either vertical or horizontal polarization measurements. Reflection errors occur if the magnitude and phase of the reflection coefficient ρ of the probe is incorrect. The more difficult errors

originate from insufficient knowledge of the surface currents induced on the external waveguide surface.

Other errors are encountered if the probe is not accurately positioned with respect to the sampling plane. For an accuracy of $\lambda/100$, or 0.2%, the probe location on the sampling plane requires the probe location in the z-direction, or z_o, to be less than 0.02 cm at 60 GHz. This frequency will be the highest frequency for a near-field range to be completed by 1987. Tolerance in angular alignment depends on the smoothness of the test antenna's far-field pattern. If $\Delta\theta$ is the error tolerance, then

$$\frac{dG/d\theta}{10\log\theta}\,\Delta\theta < 0.002 \text{ radian}, \tag{34}$$

where $G(\theta)$ is the antenna voltage gain in dB. For example, a cosine gain pattern at $\theta = 45°$ has

$$\frac{dG}{d\rho} = -10\log\theta, \tag{35}$$

so that $\Delta\theta \approx 0.002$ radian, or 0.1 degree.

Other errors due to mechanical vibrations and bending of the probe antenna carrier are being investigated for a near-field range with a 60 meter by 60 meter sampling plane and a frequency of 60 GHz.

REFERENCES

[1] Kerns, D.M., "Plane-Wave Scattering Matrix Theory of Antenna and Antenna-Antenna Interaction," National Bureau of Standards Monograph 162, June 1981.

[2] Baird, R.C., et al., "Recent Experimental Results in Near Field Antenna Measurements," Electron. Lett., Vol. 6, pp. 349-351, May 1970.

[3] Joy, E.B. and D.T. Paris, "Spatial Sampling and Filtering in Near-Field Measurements," IEEE Trans., vol. AP-20, pp. 253-261, May 1972.

[4] Newell, A.C. and M.L. Crawford, "Planar Near Field Measurements on High Performance Array Antennas," National Bureau of Standards Report NBSIR 74-380, July 1974.

[5] Brown, J. and E.V. Jull, "The Prediction of Aerial Radiation Patterns from Near Field Measurements," Journal II, vol. 108B, pp. 635-644, November 1961.

[6] Leach, W.M., Jr. and D.T. Paris, "Probe Compensated Near-Field Measurements on a Cylinder," IEEE Trans., vol. AP-21, pp. 435-445, July 1973.

[7] Wacker, P.F., "Non-Planar Near Field Measurements: Spherical Scanning," National Bureau of Standards Report NBSIR 75-809, June 1975.

[8] "IEEE Test Procedure for Antennas, Number 149 (Revision of 48 IRE 282) January 1965," IEEE Trans., vol. AP-13, pp. 347-446, May 1965.

[9] Balanis, C.A., Antenna Theory Analysis and Design, New York: Harper and Row, 1982.

[10] Paris, D.T., W.M. Leach, Jr., and E.B. Joy, "Basic Theory of Probe-Compensated Near-Field Measurements," IEEE Trans., vol. AP-26, pp. 373-379, May 1978.

[11] Joy, E.B., W.M. Leach, Jr., G.P. Rodrigue and D.T. Paris, "Applications of Probe-Compensated Near-Field Measurements," IEEE Trans., vol. AP-26, pp. 379-389, May 1978.

[12] Biggs, A.W., "Asymptotic Approximations for Surface Scattering Integrals," IEEE Trans., vol. AP-15, pp. 443-445, May 1977.

[13] Collin, R.E. and F.J. Zucker, Antenna Theory, Part I, New York: McGraw Hill, Chapter 4, 1969.

[14] Richmond, J.H. and T.E. Tice, "Probes for Microwave Near-Field Measurements," IEEE Trans., vol. MTT-3, pp. 32-34, April 1955.

END

FILMED

4-85

DTIC